Biophysical Chemistry, 48 (1993) 301–313
Elsevier Science Publishers B.V., Amsterdam

BIOCHE 01806

Specifying bounds on the rate constants of intramolecular two-state excited-state processes by global compartmental analysis of the fluorescence decay surface

Noël Boens [a,*], Luc Van Dommelen [a] and Marcel Ameloot [b]

[a] *Department of Chemistry, Katholieke Universiteit Leuven, B-3001 Heverlee (Belgium)*
[b] *Limburgs Universitair Centrum, B-3590 Diepenbeek (Belgium)*

Abstract

This report is an extension of the identifiability study [Boens et al., *J. Phys. Chem.* 96 (1992) 6331–6342] of intramolecular two-state excited-state processes. The identifiability study is expressed in terms of the rate constants and the parameters $\tilde{b}_1$ and $\tilde{c}_1$, where $\tilde{b}_1$ is the relative absorbance of ground-state species 1 and $\tilde{c}_1$ is the normalized spectral emission weighting factor of the corresponding excited-state species 1*. From the decay times and the preexponential factors of a single fluorescence decay trace, it is generally possible to derive two sets of rate constants when one rate constant, $\tilde{b}_1$ and $\tilde{c}_1$ are known beforehand. A unique set of rate constants can be obtained when one rate constant is known in combination with the following sets of values for ($\tilde{b}_1$, $\tilde{c}_1$): (0.5, 1), (0.5, 0), (1, 0.5), (0, 0.5), (0.5, 0.5), (1, 1) or (0, 0). It is further shown that when ($\tilde{b}_1$, $\tilde{c}_1$) equals (1, 1) or (0, 0), i.e. a single species is excited and the fluorescence of only that species is observed, upper and lower bounds on all rate constants can be specified without any *a priori* information about the rate constant values. The bounds on the rate constants can be specified in terms of the decay times and the preexponential factors estimated from the biexponential analysis of a single fluorescence decay trace with $\tilde{b}_1 = 1$ and $\tilde{c}_1 = 1$ or, equivalently, $\tilde{b}_1 = 0$ and $\tilde{c}_1 = 0$. This analysis approach can provide kinetic information of intramolecular electron transfer and exciplex formation when no suitable model compound is available.

Keywords: Intramolecular two-state excited-state processes; Fluorescence decay surface; Rate constants; Kinetic analysis; Global compartmental analysis approach

1. Introduction

Time-resolved fluorometry in the time [1,2] and frequency domain [3,4] is the ideal technique to unravel the often complex kinetics of excited-state processes. The measurement of the multidimensional fluorescence decay surface as a function of various experimental conditions provides data with high accuracy allowing an elaborate data analysis. The analysis of all related experimental fluorescence decay traces in a single step is the most appropriate way to discriminate between competing kinetic models and to obtain the most reliable parameter estimates. In this so-called global analysis approach [5–8] parameters can be linked over various decay traces. The power and performance of this simultaneous analysis has been extensively demonstrated [5–8]. In many cases the time relaxation of the excited

* To whom correspondence should be addressed.

system can be described by a sum of exponentially decaying functions. The parameters of interest are not the decay times and the corresponding preexponential factors (these may be called descriptive or empirical parameters) but rather the rate constants and the species-associated spectra. To benefit the most of the merits of this global analysis approach, one has to fit for the underlying parameters, i.e. the rate constants which can be linked indeed. Therefore, a compartmental description of the processes is necessary [9,10]. The implementation of global compartmental analysis [11–19] has the additional advantage that the parameters of interest are determined directly from the complete decay data surface in a single step. In a recent paper [18] we discussed the global compartmental analysis of the fluorescence decay surface of intramolecular two-state excited-state processes. The kinetic equations specifying the fluorescence decay and the time-course of the two excited-state species concentrations were derived in terms of the rate constants k_{ij}, and the spectroscopic parameters $\tilde{b}_1$ and $\tilde{c}_1$, where $\tilde{b}_1$ is the relative absorbance of ground-state species 1 and $\tilde{c}_1$ is the normalized spectral emission weighting factor of the corresponding excited-state species 1*. It was shown that at least three (kinetic and/or spectroscopic) parameters of the intramolecular two-state excited-state process must be known beforehand to recover all relevant kinetic and spectroscopic information. These three parameters can be either (a) two rate constants and one spectroscopic parameter [(1) two k_{ij} and one $\tilde{b}_1$, (2) two k_{ij} and one $\tilde{c}_1$], or (b) one rate constant and two spectroscopic parameters [(3) one k_{ij}, one $\tilde{b}_1$ and one $\tilde{c}_1$, (4) one k_{ij} and two $\tilde{b}_1$, (5) one k_{ij} and two $\tilde{c}_1$], or (c) three spectroscopic parameters [(6) two $\tilde{b}_1$ and one $\tilde{c}_1$, (7) one $\tilde{b}_1$ and two $\tilde{c}_1$, (8) three $\tilde{b}_1$, (9) three $\tilde{c}_1$]. The conditions (1)–(3) require at least one fluorescence decay trace. A minimum of two decay traces is needed for conditions (4)–(7), while at least three fluorescence decays are necessary for conditions (8) and (9). The situation (b) where one rate constant and two spectroscopic parameters are assumed to be known is frequently encountered when an appropriate model compound is available. One postulates that the value of k_{0j} measured for the model compound is transferable to the intramolecular excited-state process. Conditions (6) to (9) indicate that spectroscopic information alone can suffice for the system to be identifiable. In these cases a model compound is not essential.

This paper is an extension of a previous study of intramolecular two-state excited-state processes [18]. As this report describes a compartmental approach to the kinetics of excited-state processes, we shall first define the term "compartmental system" in photophysics. The second part presents the matrix description of the kinetics of excited-state concentrations and fluorescence. In the third part we shall define the conditions under which the rate constants are uniquely defined for the case where one k_{ij}, and specific values of one $\tilde{b}_1$ and one $\tilde{c}_1$ are known. It will be shown that, when ($\tilde{b}_1 = 1$, $\tilde{c}_1 = 1$) or ($\tilde{b}_1 = 0$, $\tilde{c}_1 = 0$), upper and lower limits on all rate constants k_{ij} can be specified in the absence of any other information. By using computer-generated fluorescence decay traces, it will be demonstrated how these upper and lower bounds on the rate constants can be determined. At last, the bounds on the rate constants will be expressed in terms of the decay times and the corresponding preexponential factors estimated from the biexponential analysis of a single decay curve with ($\tilde{b}_1 = 1$, $\tilde{c}_1 = 1$) or, equivalently, ($\tilde{b}_1 = 0$, $\tilde{c}_1 = 0$).

2. Definition of the term "compartment"

In photophysics a compartment is composed of a distinct type of species which acts kinetically in a unique way. The concentration of the constituting species can change when the compartments exchange material through an intramolecular or intermolecular process. Compartments can be divided into ground and excited state compartments depending upon the state of the composing species. An excited-state system can be viewed as a compartmental system made up of a number of excited-state compartments. There may be inputs from the ground-state compartments into one or more of the excited-state compartments by light excitation. There is output from the excited-state

compartments to the environment by deactivation such as fluorescence, internal conversion, intersystem crossing, etc. If the concentrations of the species in the ground state do not significantly change upon excitation, it suffices to consider the excited-state compartments only. In that case, the photophysical system can be regarded as open. A compartmental system can be closed by adding the ground-state compartments corresponding to the excited-state compartments. Compartments are usually depicted as boxes (see Scheme 1), which enclose the composing species. Single-headed arrows pointing away from a compartment are used to represent outflow from that compartment, whereas single-headed arrows pointing toward a compartment depict inflow into that compartment.

3. Kinetics

Consider a causal, linear, time-invariant, intramolecular system consisting of two distinct types of excited-state species (Scheme 1). Ground-state species 1 can reversibly convert to ground-state species 2. Excitation by light creates the excited-state species 1* and 2*, which can decay by fluorescence, internal conversion and intersystem crossing. The composite rate constants for those processes are denoted by k_{01} and k_{02}. The rate constant describing the transformation $1^* \rightarrow 2^*$ is represented by k_{21}, whereas k_{12} characterizes the transformation $2^* \rightarrow 1^*$.

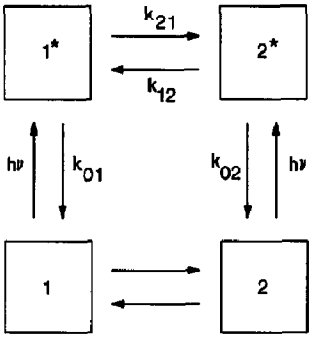

Scheme 1.

If the system depicted in Scheme 1 is excited by a δ-pulse which does not significantly alter the concentrations of the ground-state species, the concentration dependence of the two excited species 1* and 2* as a function of time is described by the following matrix equation:

$$\mathbf{X}^{*\prime}(t) = \mathbf{A}\mathbf{X}^*(t), \qquad t \geq 0 \tag{1}$$

where $\mathbf{A}$, $\mathbf{X}^*(t)$ and $\mathbf{X}^{*\prime}(t)$ are defined as

$$\mathbf{A} \equiv \begin{bmatrix} -(k_{01}+k_{21}) & k_{12} \\ k_{21} & -(k_{02}+k_{12}) \end{bmatrix} \tag{2}$$

$$\mathbf{X}^*(t) \equiv \begin{bmatrix} [1^*](t) \\ [2^*](t) \end{bmatrix} \tag{3}$$

$$\mathbf{X}^{*\prime}(t) \equiv \frac{\mathrm{d}\mathbf{X}^*(t)}{\mathrm{d}t} \equiv \begin{bmatrix} \dfrac{\mathrm{d}[1^*]}{\mathrm{d}t} \\ \dfrac{\mathrm{d}[2^*]}{\mathrm{d}t} \end{bmatrix} \tag{4}$$

The initial conditions are defined by eq (5).

$$\mathbf{X}^*(0) \equiv \boldsymbol{b} \equiv \begin{bmatrix} b_1 \\ b_2 \end{bmatrix} \equiv \begin{bmatrix} [1^*](0) \\ [2^*](0) \end{bmatrix} \tag{5}$$

Note that $\boldsymbol{b}$ is dependent on the excitation wavelength λ^{ex}. If the compartmental matrix $\mathbf{A}$ has two distinct eigenvalues γ_1 and γ_2 with corresponding eigenvectors U_1 and U_2, the solution of the system of differential eqs. (1) is given by [20]

$$\mathbf{X}^*(t) = \boldsymbol{U} \exp(t\boldsymbol{\Gamma})\boldsymbol{U}^{-1}\boldsymbol{b}, \qquad t \geq 0 \tag{6}$$

with $\boldsymbol{U} = [U_1, U_2]$ and $\boldsymbol{U}^{-1}$ the inverse of $\boldsymbol{U}$, and $\exp(t\boldsymbol{\Gamma}) = \mathrm{diag}\{\exp(\gamma_1 t), \exp(\gamma_2 t)\}$.

The fluorescence δ-response function, $f(\lambda^{em}, \lambda^{ex}, t)$, measured at emission wavelength λ^{em} due to excitation at λ^{ex} is expressed by

$$f(\lambda^{em}, \lambda^{ex}, t) = \boldsymbol{c}\mathbf{X}^*(t) = \boldsymbol{c}(\lambda^{em})\boldsymbol{U}\exp(t\boldsymbol{\Gamma})\boldsymbol{U}^{-1}\boldsymbol{b}(\lambda^{ex}), \quad t \geq 0 \tag{7}$$

where $\boldsymbol{c}$ is the 1×2 vector of spectral emission weighting factors $c_i(\lambda^{em})$ given by

$$c_i(\lambda^{em}) = k_{Fi}\int_{\Delta\lambda^{em}} \rho_i(\lambda^{em})\, \mathrm{d}\lambda^{em} \tag{8}$$

k_{Fi} is the fluorescence rate constant of species i^*; $\rho_i(\lambda^{em})$ is the spectral emission density of species i^* at λ^{em}, normalized to the complete steady-state fluorescence spectrum of species i^*; $\Delta\lambda^{em}$ is the emission wavelength interval where the fluorescence is monitored. The spectral emission density of species i^* at λ^{em}, $\rho_i(\lambda^{em})$, is defined by

$$\rho_i(\lambda^{em}) = F_{si}(\lambda^{em}) / \int F_{si}(\lambda^{em})\, d\lambda^{em} \tag{9}$$

where the integration extends over the whole steady-state fluorescence spectrum of species i^*.

After normalization of the elements b_i of $\boldsymbol{b}$ and c_i of $\boldsymbol{c}$ according to eq. (10),

$$\tilde{b}_i = b_i / \sum_j b_j \tag{10a}$$

$$\tilde{c}_i = c_i / \sum_j c_j \tag{10b}$$

eq. (7) can be written as

$$f(\lambda^{em}, \lambda^{ex}, t) = \kappa \tilde{\boldsymbol{c}}(\lambda^{em}) \boldsymbol{U} \exp(t\boldsymbol{\Gamma}) \boldsymbol{U}^{-1} \tilde{\boldsymbol{b}}(\lambda^{ex}), \quad t \geq 0 \tag{11}$$

with κ a proportionality constant. $\tilde{\boldsymbol{b}}(\lambda^{ex})$ can be linked over decay curves collected at the same emission wavelength, whereas $\tilde{\boldsymbol{c}}(\lambda^{em})$ can be linked over decay curves obtained at the same excitation wavelength. In our implementation of global compartmental analysis one fits directly for the rate constants k_{ij}, the normalized zero-time concentrations $\tilde{b}_1$ and the normalized spectral emission weighting factors $\tilde{c}_1$.

Equation (11) can be written as a sum of two exponential terms:

$$f(\lambda^{em}, \lambda^{ex}, t) = \alpha_1(\lambda^{em}, \lambda^{ex}) \exp(\gamma_1 t) + \alpha_2(\lambda^{em}, \lambda^{ex}) \exp(\gamma_2 t), \quad t \geq 0 \tag{12}$$

The exponential factors $\gamma_{1,2}$ are related to the decay times $\tau_{1,2}$ according to

$$\gamma_{1,2} = -1/\tau_{1,2} \tag{13}$$

and are given by

$$\gamma_{1,2} = -\tfrac{1}{2}\left\{S_1 + S_2 \mp \left[(S_1 - S_2)^2 + 4P\right]^{1/2}\right\} \tag{14}$$

with

$$S_1 = k_{01} + k_{21} \tag{15a}$$

$$S_2 = k_{02} + k_{12} \tag{15b}$$

$$P = k_{21} k_{12} \tag{15c}$$

The preexponential terms α_1 and α_2 are

$$\alpha_1 = \kappa(\tilde{c}_1 \beta_{11} + \tilde{c}_2 \beta_{21}) \tag{16a}$$

$$\alpha_2 = \kappa(\tilde{c}_1 \beta_{12} + \tilde{c}_2 \beta_{22}) \tag{16b}$$

with

$$\beta_{11} = \left[\tilde{b}_1(S_1 + \gamma_2) - \tilde{b}_2 k_{12}\right] / (\gamma_2 - \gamma_1) \tag{17a}$$

$$\beta_{12} = -\left[\tilde{b}_1(S_1 + \gamma_1) - \tilde{b}_2 k_{12}\right] / (\gamma_2 - \gamma_1) \tag{17b}$$

$$\beta_{21} = \left[\tilde{b}_2(S_2 + \gamma_2) - \tilde{b}_1 k_{21}\right] / (\gamma_2 - \gamma_1) \tag{17c}$$

$$\beta_{22} = -\left[\tilde{b}_2(S_2 + \gamma_1) - \tilde{b}_1 k_{21}\right] / (\gamma_2 - \gamma_1) \tag{17d}$$

and

$$\tilde{b}_2 = 1 - \tilde{b}_1 \tag{18a}$$

$$\tilde{c}_2 = 1 - \tilde{c}_1 \tag{18b}$$

4. Identifiability

The following formulas are available for relating the parameters of the fluorescence δ-response function $f(t)$ to the unknown system parameters k_{ij}, $\tilde{b}_1$ and $\tilde{c}_1$. The functions σ_1 and σ_2 are defined as [9]

$$\sigma_1 = \gamma_1 + \gamma_2 = -k_{01} - k_{21} - k_{02} - k_{12} = -S_1 - S_2 \tag{19}$$

$$\sigma_2 = \gamma_1 \gamma_2 = k_{01} k_{02} + k_{01} k_{12} + k_{02} k_{21} = k_{01} S_2 + k_{02} k_{21} = k_{02} S_1 + k_{01} k_{12} = S_1 S_2 - P \tag{20}$$

The Markov parameters m_0 and m_1 [9] are given by

$$m_0 = \kappa\left(\tilde{c}_1\tilde{b}_1 + \tilde{c}_2\tilde{b}_2\right) \tag{21a}$$

$$m_1 = \kappa\left\{-\tilde{c}_1\tilde{b}_1(k_{01}+k_{21}) + \tilde{c}_1\tilde{b}_2k_{12} + \tilde{c}_2\tilde{b}_1k_{21} - \tilde{c}_2\tilde{b}_2(k_{02}+k_{12})\right\} \tag{21b}$$

For a decay trace collected at emission wavelength λ^{em} due to excitation at λ^{ex}, elimination of the scaling factor κ from eqs. (21) leads to

$$Ak_{01} + Bk_{21} + Ck_{02} + Dk_{12} = E \tag{22}$$

with

$$A \equiv \tilde{b}_1\tilde{c}_1 \tag{23a}$$

$$B \equiv \tilde{b}_1(2\tilde{c}_1 - 1) \tag{23b}$$

$$C \equiv \left(\tilde{b}_1 - 1\right)\left(\tilde{c}_1 - 1\right) \tag{23c}$$

$$D \equiv \left(\tilde{b}_1 - 1\right)(2\tilde{c}_1 - 1) \tag{23d}$$

$$E \equiv (m_1/m_0)\left(-2\tilde{b}_1\tilde{c}_1 + \tilde{b}_1 + \tilde{c}_1 - 1\right) \tag{23e}$$

Note that A, B, C, D and E depend on the excitation and emission wavelengths. For a single decay trace collected at emission wavelength λ^{em} due to excitation at λ^{ex}, eqs. (19), (20) and (22) (eqs. 23 inclusive) are the three equations from which the four rate constants k_{ij}, $\tilde{b}_1$ and $\tilde{c}_1$ must be derived. The bicompartmental system depicted by Scheme 1 is not identifiable, because only three independent equations are available.

Equation (22) can only be constructed when m_0 of the considered fluorescence decay is different from zero; $m_0 = 0$ if (1) $\tilde{b}_1 = 1$ and $\tilde{c}_1 = 0$, or (2) $\tilde{b}_1 = 0$ and $\tilde{c}_1 = 1$ [18]. In that case we have that $\alpha_1 = -\alpha_2$, and as a consequence, a fluorescence decay with $\alpha_1/\alpha_2 = -1$ will not provide extra useful kinetic information. Equation (22) can be substantially simplified for specific sets of $(\tilde{b}_1, \tilde{c}_1)$.

If one rate constant value is known, a single decay trace measured at λ^{em} (with known $\tilde{c}_1$) due to excitation at λ^{ex} (with known $\tilde{b}_1$) can suffice to determine all relevant system parameters. It should be emphasized that in all cases mathematically two solutions are possible for each rate constant k_{ij}. The condition of nonnegativity for k_{ij} may yield the unique solution for the rate constants.

We shall now identify the cases where unique solutions for the rate constants are obtained.

(1) If $\tilde{b}_1 = 0.5$ and $\tilde{c}_1 = 1$, unique values for k_{01}, k_{21} and k_{02} (k_{12}, respectively) are obtained only in the case when k_{12} (k_{02}, respectively) is known.

(2) If $\tilde{b}_1 = 0.5$ and $\tilde{c}_1 = 0$, unique values for k_{02}, k_{12} and k_{01} (k_{21}, respectively) are obtained only in the case when k_{21} (k_{01}, respectively) is known.

(3) If $\tilde{b}_1 = 1$ and $\tilde{c}_1 = 0.5$, k_{01} is uniquely determined. Unique values for the remaining rate constant are obtained when k_{21} or k_{02} are known.

(4) If $\tilde{b}_1 = 0$ and $\tilde{c}_1 = 0.5$, k_{02} is uniquely determined. Unique values for the remaining rate constant are obtained when k_{12} or k_{01} are known.

(5) If $\tilde{b}_1 = 0.5$ and $\tilde{c}_1 = 0.5$, unique values for k_{12}, k_{21} and k_{01} (k_{02}, respectively) are obtained when k_{02} (k_{01}, respectively) is known.

(6) The case $\tilde{b}_1 = 1$ and $\tilde{c}_1 = 1$ will now be described in detail. If $\tilde{b}_1 = 1$ and $\tilde{c}_1 = 1$, eq. (22) reduces to

$$S_1 = -m_1/m_0 \tag{24}$$

Combining eq. (24) with eq. (19) leads to

$$S_2 = -\sigma_1 + m_1/m_0 \tag{25}$$

From eq. (20) we have that

$$P = -\left[(-\sigma_1 + m_1/m_0)(m_1/m_0) + \sigma_2\right] \tag{26}$$

If one rate constant is known, eqs. (15), (24), (25) and (26) allow us to calculate the values of three remaining rate constants.

When k_{01} is known, the values of k_{21}, k_{12}, and k_{02} are given by

$$k_{21} = S_1 - k_{01} \tag{27}$$

$$k_{12} = P/k_{21} \tag{28}$$

$$k_{02} = S_2 - k_{12} \tag{29}$$

When k_{21} is known, the values of k_{12} and k_{02} are given by eqs. (28) and (29), respectively, and k_{01} is obtained from S_1.

When k_{02} is known, the values for k_{12}, k_{21}, and k_{01} are given by

$$k_{12} = S_2 - k_{02} \tag{30}$$

$$k_{21} = P/k_{12} \tag{31}$$

$$k_{01} = S_1 - k_{21} \tag{32}$$

When k_{12} is known, the values of k_{21} and k_{01} are given by eqs. (31) and (32), respectively, and k_{02} is obtained from S_2. Note that, irrespective of which rate constant is known, unique values for all rate constants are obtained.

If $\tilde{b}_1 = 1$, $\tilde{c}_1 = 1$ and no rate constant values are known beforehand, upper ("max") and lower ("min") limits on the rate constants can be set. The only condition for specifying these bounds is that one parameter value of the set $\{k_{01}^{\min}, k_{21}^{\max}, k_{02}^{\max}, k_{12}^{\min}\}$ and one parameter value of the set $\{k_{01}^{\max}, k_{21}^{\min}, k_{02}^{\min}, k_{12}^{\max}\}$ are known. Suppose that $k_{01}^{\min}$ is known. $k_{21}^{\max}$ is calculated from eq. (27) by substituting $k_{01}^{\min}$ for k_{01}. Substitution of $k_{21}^{\max}$ in eq. (28) yields $k_{12}^{\min}$, and eq. (29) yields $k_{02}^{\max}$ when k_{12} is replaced by $k_{12}^{\min}$. Similarly, the knowledge of $k_{02}^{\min}$ allows us to calculate $k_{12}^{\max}$ from eq. (30). Equation (31) yields $k_{21}^{\min}$, while eq. (32) gives $k_{01}^{\max}$ when $k_{21} = k_{21}^{\max}$.

Without any information about rate constant limits one can arbitrarily set $k_{01}^{\min} = 0$ and $k_{02}^{\min} = 0$. In that way one obtains the widest possible (that is extreme) limits on the rate constants. When $k_{01}^{\min}$ and $k_{02}^{\min}$ are both equal to zero, the limits on the rate constants are

$$0 < k_{01} < S_1 - P/S_2 \tag{33a}$$

$$P/S_2 < k_{21} < S_1 \tag{33b}$$

$$0 < k_{02} < S_2 - P/S_1 \tag{33c}$$

$$P/S_1 < k_{12} < S_2 \tag{33d}$$

Note that the case $\tilde{b}_1 = 0$ and $\tilde{c}_1 = 0$ is completely analogous with the case $\tilde{b}_1 = 1$ and $\tilde{c}_1 = 1$.

5. Parameter estimation

5.1. Program implementation

The global compartmental analysis of the fluorescence decay surface of species undergoing excited-state processes was implemented in the existing general global analysis program [8] based on Marquardt's algorithm [21].

Consider the intramolecular two-state excited-state process depicted by Scheme 1. The global fitting parameters are k_{01}, k_{21}, k_{02}, k_{12}, $\tilde{b}_1(\lambda^{ex})$ and $\tilde{c}_1(\lambda^{em})$. Assigning initial guesses to the rate constants k_{01}, k_{21}, k_{02}, k_{12} allows one to construct the compartmental matrix A for each decay trace. The eigenvalues γ and the associated eigenvectors of this matrix are determined using routines from EISPACK, Matrix Eigensystem Routines [22]. The eigenvectors are then scaled to the initial conditions $\tilde{b}$ and the preexponential factors are computed. The fluorescence response of the sample is then calculated. Using this approach, experiments done at different excitation/emission wavelengths and at multiple timing calibrations are linked by all rate constants defining the system.

The fitting parameters were determined by minimizing the *global reduced* chi-square χ_g^2:

$$\chi_g^2 = \sum_{\ell}^{q} \sum_{i} w_{\ell i} \left(y_{\ell i}^{o} - y_{\ell i}^{c} \right)^2 / \nu \tag{34}$$

where the index ℓ sums over q experiments and the index i sums over the appropriate channel limits for each individual experiment. $y_{\ell i}^{o}$ and $y_{\ell i}^{c}$ denote respectively the observed (experimentally measured or synthetic) and calculated (fitted) values corresponding to the ith channel of the ℓth experiment, and $w_{\ell i}$ is the corresponding statistical weight. ν represents the number of degrees of freedom for the entire multidimensional fluorescence decay surface. The quality of the fits was judged by the value of the global reduced chi-square statistic χ_g^2 and its corresponding $Z_{\chi_g^2}$,

$$Z_{\chi_g^2} = \left(\tfrac{1}{2}\nu\right)^{1/2} \left(\chi_g^2 - 1\right) \tag{35}$$

By using $Z_{\chi_g^2}$ the goodness of fit of analyses with different ν can be readily compared. Fits with $Z_{\chi_g^2} > 5$ were considered to be unacceptable. The additional statistical criteria to assess the quality of the fit are described elsewhere [2].

5.2. Synthetic data generation

Synthetic sample decays were generated by convolution of $f(t)$ with a nonsmoothed mea-

sured instrument response function. The preexponential terms α_i and corresponding eigenvalues γ_i of the biexponential decays were computed from the rate constants k_{ij}, $\tilde{b}_1$ and $\tilde{c}_1$ by a dedicated computer program. The preexponential terms were adjusted to obtain the desired number of counts. All computer simulated decays had $\frac{1}{2}$K data points with approximately 10^4 counts in the peak channel. The time increment per channel (50 ps) was chosen to ensure that the number of counts in the final channels was about 5% or less of the peak channel counts. Full details of the decay data simulations are given elsewhere [23]. The synthetic data generations and all individual and global analyses were done on an IBM RISC System/6000 computer.

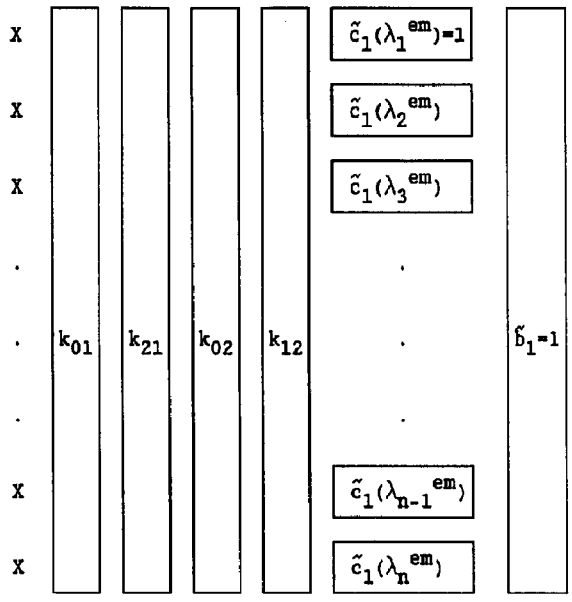

Scheme 2.

6. Specifying bounds on the rate constants by global compartmental analysis of computer-generated decays with $\tilde{b}_1 = 1$ and $\tilde{c}_1 = 1$

To specify upper and lower limits on the rate constants for the case with $\tilde{b}_1 = 1$ and $\tilde{c}_1 = 1$, computer-generated decay traces were used. The simulation values of the rate constants were: $k_{01} = 0.2$ (ns)$^{-1}$, $k_{21} = 0.3$ (ns)$^{-1}$, $k_{02} = 0.1$ (ns)$^{-1}$, and $k_{12} = 0.8$ (ns)$^{-1}$, corresponding to decay times $-\gamma_1^{-1} = 0.81$ ns and $-\gamma_2^{-1} = 5.85$ ns, and $S_1 = 0.5$ (ns)$^{-1}$, $S_2 = 0.9$ (ns)$^{-1}$, $P = 0.24$ (ns)$^{-2}$. In a first set of 11 simulated fluorescence traces $\tilde{b}_1$ was set to unity for the whole fluorescence decay surface and $\tilde{c}_1$ varied from 1.0 to 0.0 in steps of 0.1. The linking scheme used in the global compartmental analysis of this fluorescence decay surface is shown in Scheme 2. In this scheme boxed parameters are linked, whereas X denotes the unlinked scaling factors. In all analyses of this decay surface the rate constants and $\tilde{b}_1 = 1$ (constant) were linked over the entire decay surface. $\tilde{c}_1$ was kept constant at unity for the decay with $\tilde{c}_1 = 1$, whereas the $\tilde{c}_1$ parameters of the other decay traces were freely adjustable. The initial parameter guesses for the adjustable parameters were substantially different from the simulation values. In all subsequent analyses the rate constants were constrained to positive values.

In the first series of global compartmental analyses k_{01} was kept constant at preset values ranging from 0.001 (ns)$^{-1}$ to 0.25 (ns)$^{-1}$. The other rate constants were freely adjustable. Figure 1A shows $Z_{\chi_g^2}$ of the global compartmental analyses as a function of k_{01}. It is clear that $Z_{\chi_g^2}$ remains virtually constant for k_{01} smaller than 0.24 (ns)$^{-1}$. This upper bound was obtained by visual inspection. Above this value $Z_{\chi_g^2}$ increased rapidly and unacceptable fits were obtained. The rate constants k_{21}, k_{02} and k_{12} recovered at the various preset values of k_{01} are shown in Fig. 1B. The percentage errors on all estimated rate constants were always smaller than 2%. This figure indicates that k_{21} decreases with increasing k_{01}. The estimated k_{02} values decrease while the k_{12} values increase with higher k_{01}. A different picture emerged when the parameters S_1, S_2 and P were plotted as a function of k_{01} (Figs. 1C–E). For k_{01} values smaller than 0.24 (ns)$^{-1}$ plateaus could be observed for S_1, S_2 and P as a function of k_{01}. The constant values of S_1, S_2 and P were in excellent agreement with those calculated from the simulation values of the rate constants. We must emphasize that plateau values and bounds were obtained by visual inspection. When k_{01}

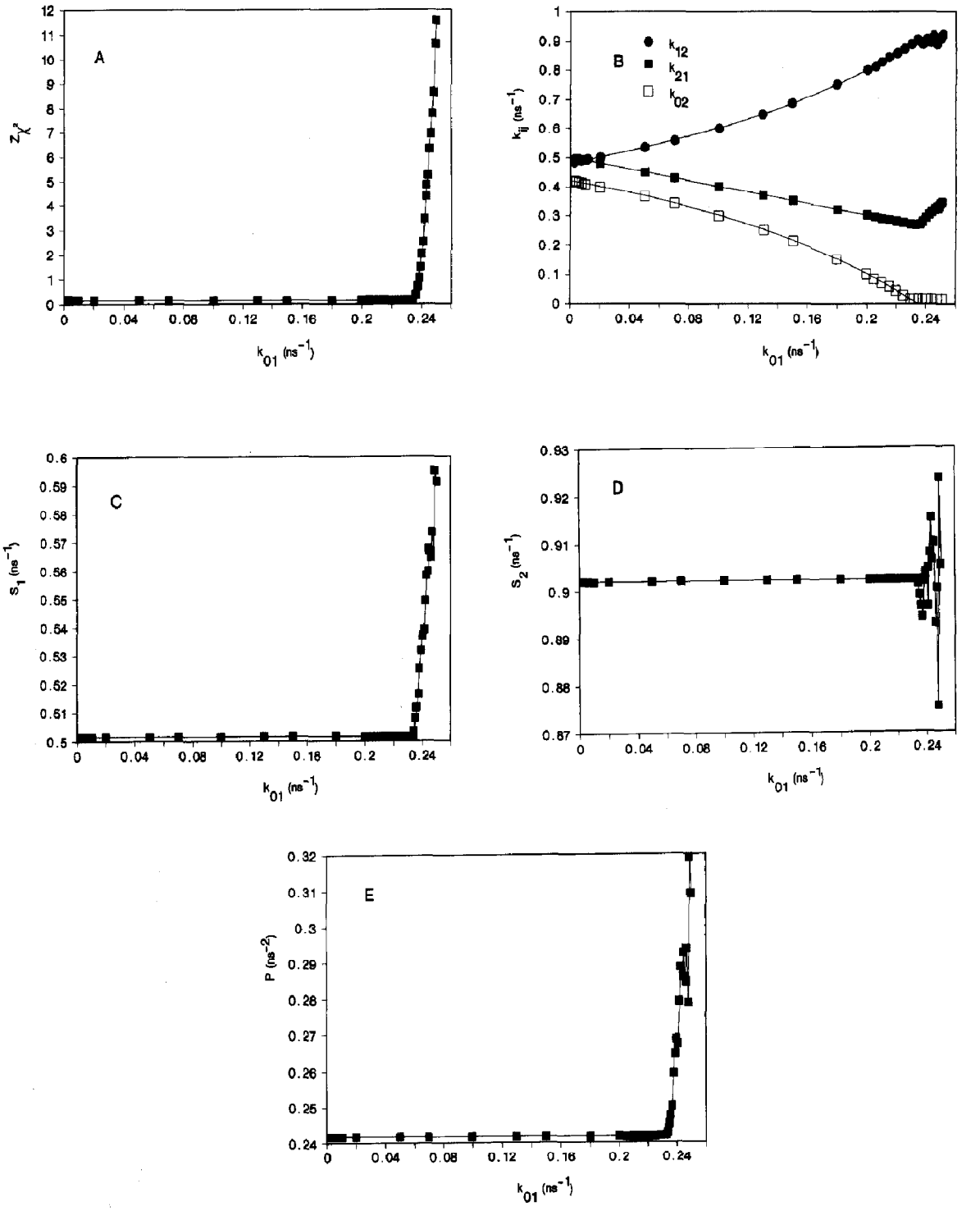

Fig. 1. (A) $Z_{\chi_g^2}$ of the global compartmental analyses of 11 decays with $\tilde{b}_1 = 1$ and $\tilde{c}_1$ varying between 1.0 and 0.0 in steps of 0.1 (Scheme 2) as a function k_{01}. (B) Globally estimated values of the rate constants k_{21}, k_{02} and k_{12} as a function of k_{01}. The standard errors on all estimated rate constants are within the plotting symbols. (C) S_1 calculated from the estimated rate constant k_{21} and the scanned rate constant k_{01} as a function of k_{01}. (D) S_2 calculated from the estimated rate constants k_{02} and k_{12} as a function of k_{01}. (E) P calculated from the estimated rate constants k_{21} and k_{12} as a function of k_{01}.

was about 0.24 $(ns)^{-1}$, S_1, S_2 and P increased. From the plots compiled in Fig. 1 it is evident that the upper limit of k_{01} is 0.24 $(ns)^{-1}$, whereas its lower limit is apparently equal to zero.

In the second series of global compartmental analyses k_{21} was scanned, i.e. kept constant at different preset values ranging from 0.2 $(ns)^{-1}$ to 0.6 $(ns)^{-1}$. All other rate constants were freely adjustable. Figure 2A shows $Z_{\chi^2_g}$ as a function of k_{21}. From this figure it is evident that adequate fits were observed only for a limited interval of k_{21} values. Indeed, $Z_{\chi^2_g}$ increased for k_{21} values smaller than 0.26 $(ns)^{-1}$ and higher than 0.51 $(ns)^{-1}$. The estimated values of the individual rate constants k_{01}, k_{02} and k_{12} varied as a function of k_{21}, in analogy with the results when k_{01} was scanned (see Fig. 2B). The values for S_1, S_2 and P calculated from the estimated rate constant values and k_{21} are plotted in Figs. 2C–E. Within the region $0.27\ (ns)^{-1} < k_{21} < 0.50\ (ns)^{-1}$ the values of S_1, S_2 and P were constant. These values define the lower and upper bounds on k_{21}. The plateau values of S_1, S_2 and P coincided with those calculated from the simulation values of the rate constants.

In the third series of global compartmental analyses the rate constant k_{02} was scanned. The results (not shown) of these analyses were very analogous with those when k_{01} was scanned. Only an upper limit on k_{02} could be defined, below which S_1, S_2 and P were constant. The upper limit on k_{02}, determined by visual examination, was found to be 0.42 $(ns)^{-1}$.

Finally, the fluorescence decay surface was analyzed with k_{12} constant at different preset values. The results (not shown) were very similar to those when k_{21} was scanned. The rate constant k_{12} had upper and lower limits: $0.48\ (ns)^{-1} < k_{12} < 0.91\ (ns)^{-1}$. Based on the scanning of the four individual rate constants we can specify the following upper and lower bounds on the rate constants: $0\ (ns)^{-1} < k_{01} < 0.23\ (ns)^{-1}$; $0.26\ (ns)^{-1} < k_{21} < 0.50\ (ns)^{-1}$; $0\ (ns)^{-1} < k_{02} < 0.42\ (ns)^{-1}$; $0.48\ (ns)^{-1} < k_{12} < 0.91\ (ns)^{-1}$. Perfect agreement was found between these bounds and those calculated according to eq. (33) using the simulation values of S_1, S_2 and P.

Instead of scanning all four rate constants it suffices to perform a series of global compartmental analyses as a function of only one rate constant. From the values of the scanned rate constant and the corresponding estimated values of the other rate constants, S_1, S_2 and P are then calculated and the limits on the rate constants can be set. The bounds on the rate constants calculated from the plateau values of S_1, S_2 and P with $k_{01}^{\min} = 0$ and $k_{02}^{\min} = 0$ matched very well those obtained by scanning all four rate constants. Indeed, the bounds obtained from the plateau values of S_1, S_2 and P with $k_{01}^{\min} = 0$ and $k_{02}^{\min} = 0$ were: $0\ (ns)^{-1} < k_{01} < 0.23\ (ns)^{-1}$; $0.27\ (ns)^{-1} < k_{21} < 0.50\ (ns)^{-1}$; $0\ (ns)^{-1} < k_{02} < 0.42\ (ns)^{-1}$; $0.48\ (ns)^{-1} < k_{12} < 0.90\ (ns)^{-1}$. These limits also were in excellent agreement with those calculated according to eq. (33) using the simulation values of S_1, S_2 and P.

As shown in the Identifiability Study, a single decay trace with $\tilde{b}_1 = 1$ and $\tilde{c}_1 = 1$ and a known rate constant suffices to uniquely determine the remaining rate constants. Upper and lower limits on all rate constants can be set by analysing this single fluorescence decay with $\tilde{b}_1$ and $\tilde{c}_1$ fixed at unity and by scanning any of the four rate constants. The plateaus observed for $Z_{\chi^2_g}$, S_1, S_2 and P as a function of the scanned rate constant for the analyses of a single decay trace were virtually identical to those for 11 decay traces (results not shown). The limits on the parameters were within experimental error the same. Since all kinetic information (rate constants) originates from the decay trace with $\tilde{b}_1 = 1$ and $\tilde{c}_1 = 1$, it is logical that the analyses of 1 and 11 decays gave the same results. Adding decays with $\tilde{b}_1 = 1$ and $\tilde{c}_1 \neq 1$ to the compartmental analysis of the decay with $\tilde{b}_1 = 1$ and $\tilde{c}_1 = 1$ has, however, the additional advantage that one can determine all $\tilde{c}_1$ values. Indeed, when $\tilde{b}_1 = 1$ and $\tilde{c}_1 \neq 1$, eqs. 22 and 23 allow us to uniquely determine $\tilde{c}_1$. The estimated $\tilde{c}_1$ values as a function of the scanned rate constant k_{21} are shown in Fig. 2F. The percentage errors on all estimated $\tilde{c}_1$ values were always smaller than 1%. The estimated values of $\tilde{c}_1$ and the rate constants, together with $\tilde{b}_1 = 1$ can then be used to decompose the steady-state fluorescence spectrum into the underlying species-associated emission spectra [13,18].

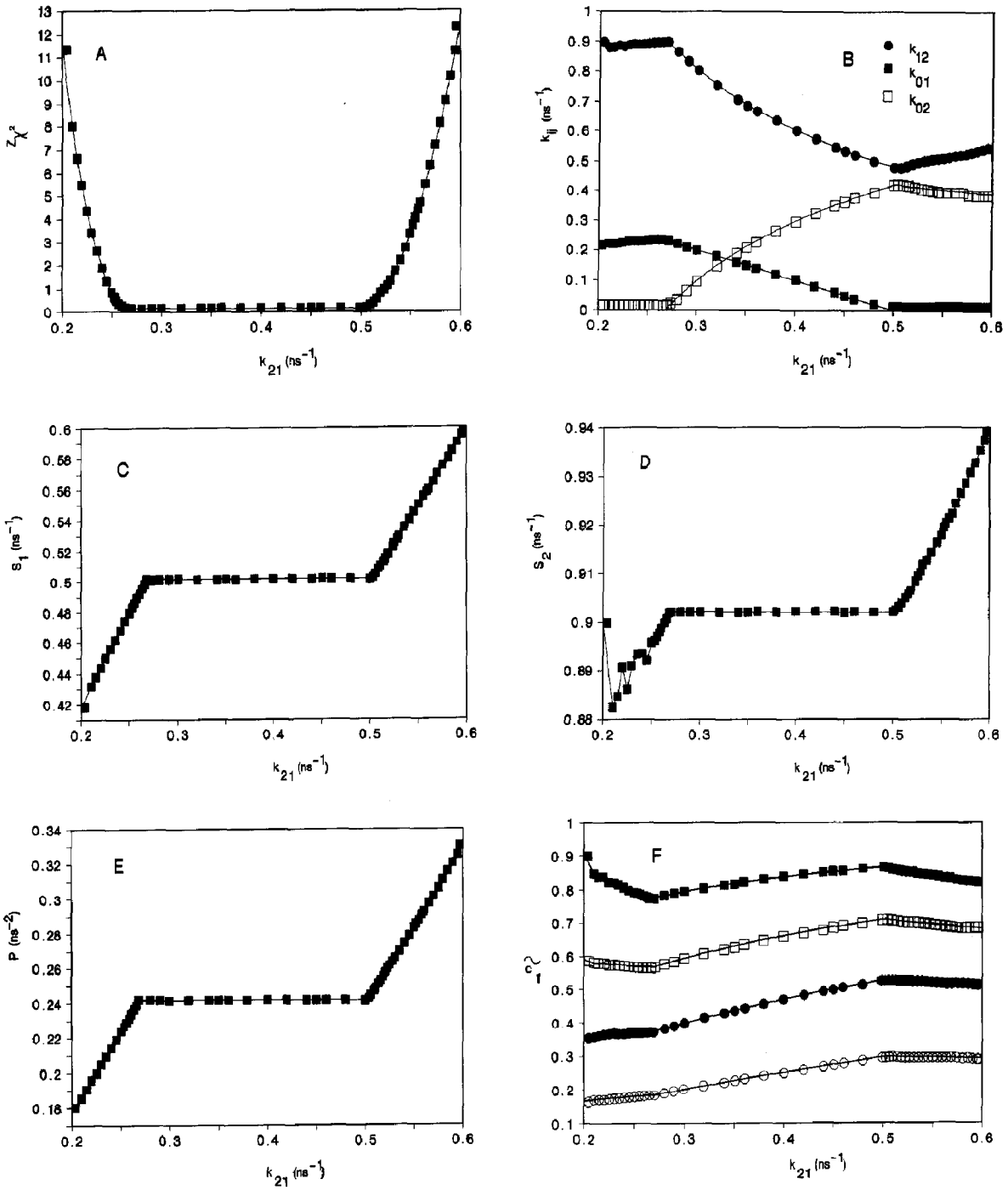

Fig. 2. (A) $Z_{\chi^2_g}$ of the global compartmental analyses of 11 decays with $\tilde{b}_1 = 1$ and $\tilde{c}_1$ varying between 1.0 and 0.0 in steps of 0.1 (Scheme 2) as a function of k_{21}. (B) Globally estimated values of the rate constants k_{01}, k_{02} and k_{12} as a function of k_{21}. The standard errors on all estimated rate constants are within the plotting symbols. (C) S_1 calculated from the estimated rate constants k_{01} and the scanned rate constant k_{21} as a function of k_{21}. (D) S_2 calculated from the estimated rate constants k_{02} and k_{12} as a function of k_{21}. (E) P calculated from the estimated rate constant k_{12} and the scanned rate constant k_{21} as a function of k_{21}. (F) Estimated $\tilde{c}_1$ values as a function of k_{21}. The simulation values of $\tilde{c}_1$ are from top to bottom 0.8 (■), 0.6 (□), 0.4 (●) and 0.2 (○). The standard errors on all estimated $\tilde{c}_1$ values are within the plotting symbols.

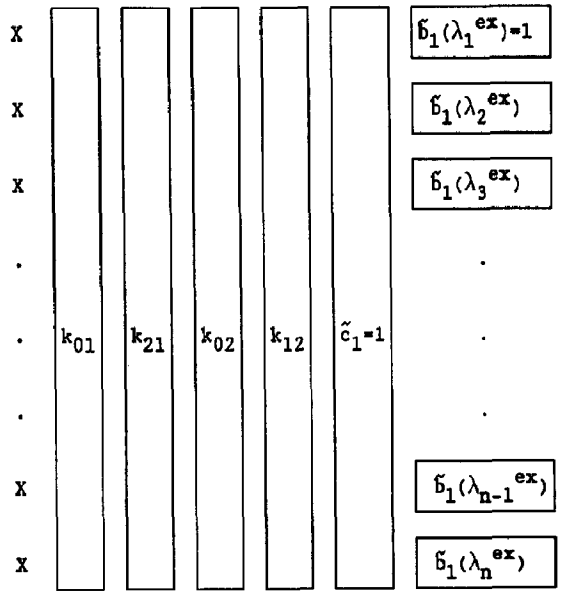

Scheme 3.

To generate a second fluorescence decay surface of 11 decay traces, we used the same rate constants as for the first decay surface. Now $\tilde{c}_1 = 1$ for all simulated decay traces and $\tilde{b}_1$ was varied from 1.0 to 0.0 in increments of 0.1. The linking scheme for the global compartmental analysis of the second fluorescence decay surface with $\tilde{c}_1 = 1$ is shown in Scheme 3. Boxed parameters are linked, whereas X denotes the unlinked scaling factors. In all subsequent analyses the rate constants and $\tilde{c}_1 = 1$ (constant) were linked over the whole decay surface. $\tilde{b}_1$ was kept constant at unity for the decay with $\tilde{b}_1 = 1$, whereas the $\tilde{b}_1$ parameters of the other decay traces were adjustable.

The analyses as a function of the individual rate constants gave results which were very similar to those of the first decay surface. The bounds on the rate constants also were comparable to those determined previously: $0\ (\text{ns})^{-1} < k_{01} < 0.24\ (\text{ns})^{-1}$; $0.26\ (\text{ns})^{-1} < k_{21} < 0.51\ (\text{ns})^{-1}$; $0\ (\text{ns})^{-1} < k_{02} < 0.43\ (\text{ns})^{-1}$; $0.48\ (\text{ns})^{-1} < k_{12} < 0.91\ (\text{ns})^{-1}$. It also is logical that the analyses of 11 decay traces gave the same results as the analyses of the single decay with $\tilde{b}_1 = 1$ and $\tilde{c}_1 = 1$. Once more this underscores the pivotal role of this decay.

7. Specifying bounds on the rate constants using the preexponential factors and the decay times of a decay with $\tilde{b}_1 = 1$ and $\tilde{c}_1 = 1$

We have shown in the sections 4 and 5 that upper and lower limits on all rate constants can be set by analysing a single fluorescence decay trace with $\tilde{b}_1 = 1$ and $\tilde{c}_1 = 1$. It suffices to keep $\tilde{b}_1$ and $\tilde{c}_1$ fixed at unity and to scan any of the four rate constants. The pivotal role of this decay was further shown in the global compartmental analysis of the decay surface where decays with $\tilde{c}_1 \neq 1$ were added to the decay with $\tilde{c}_1 = 1$. This procedure allows one to estimate all $\tilde{c}_1$ values and thus to decompose the steady-state fluorescence spectrum into its composing species-associated emission spectra. However, such a global compartmental analysis is not necessary to determine the bounds on the rate constants. Indeed, only one decay with $\tilde{b}_1 = 1$ and $\tilde{c}_1 = 1$ is needed, and rate constant limits can be specified by a simple biexponential analysis of this decay.

When $\tilde{b}_1 = 1$ and $\tilde{c}_1 = 1$, S_1, S_2 and P (eqs. 15a–c) can be expressed as a function of the preexponential terms α_i (eqs. 16a–b) and the decay times τ_i (eq. 13). S_1, S_2 and P are explicitly given be eqs. (36a–c).

$$S_1 = \frac{\alpha_1\tau_2 + \alpha_2\tau_1}{\tau_1\tau_2(\alpha_1 + \alpha_2)} \tag{36a}$$

$$S_2 = \frac{\alpha_1\tau_1 + \alpha_2\tau_2}{\tau_1\tau_2(\alpha_1 + \alpha_2)} \tag{36b}$$

$$P = \frac{\alpha_1\alpha_2(\tau_2 - \tau_1)^2}{\tau_1^2\tau_2^2(\alpha_1 + \alpha_2)^2} \tag{36c}$$

When $k_{01}^{\min}$ and $k_{02}^{\min}$ are both equal to zero, the limits on the rate constants can be expressed as a function of α_i and τ_i:

$$0 < k_{01} < \frac{\alpha_1 + \alpha_2}{\alpha_1\tau_1 + \alpha_2\tau_2} \tag{37a}$$

$$\frac{\alpha_1\alpha_2(\tau_2 - \tau_1)^2}{(\alpha_1 + \alpha_2)\tau_1\tau_2(\alpha_1\tau_1 + \alpha_2\tau_2)} < k_{21} < \frac{\alpha_1\tau_2 + \alpha_2\tau_1}{\tau_1\tau_2(\alpha_1 + \alpha_2)} \tag{37b}$$

$$0 < k_{02} < \frac{\alpha_1 + \alpha_2}{\alpha_1\tau_2 + \alpha_2\tau_1} \tag{37c}$$

$$\frac{\alpha_1\alpha_2(\tau_2 - \tau_1)^2}{(\alpha_1 + \alpha_2)\tau_1\tau_2(\alpha_1\tau_2 + \alpha_2\tau_1)} < k_{12} < \frac{\alpha_1\tau_1 + \alpha_2\tau_2}{\tau_1\tau_2(\alpha_1 + \alpha_2)} \tag{37d}$$

It is thus possible to specify upper and lower bounds on the rate constants of an intramolecular two-state excited-state process by using the preexponential factors and decay times estimated by the biexponential analysis of a single decay trace with $\tilde{b}_1 = 1$ and $\tilde{c}_1 = 1$.

By using the estimated values for $\alpha_1 = 0.31$, $\alpha_2 = 0.69$, $\tau_1 = 0.81$ ns, $\tau_2 = 5.85$ ns, the bounds on the rate constants calculated according to eqs. (37) were: $0\ (\text{ns})^{-1} < k_{01} < 0.23\ (\text{ns})^{-1}$; $0.27\ (\text{ns})^{-1} < k_{21} < 0.50\ (\text{ns})^{-1}$; $0\ (\text{ns})^{-1} < k_{02} < 0.42\ (\text{ns})^{-1}$; $0.48\ (\text{ns})^{-1} < k_{12} < 0.90\ (\text{ns})^{-1}$. Excellent agreement was found between these limits and those calculated according to eq. (33) using the simulation values of S_1, S_2 and P. When all 11 decay traces were analyzed simultaneously in terms of α_i and τ_i with the decay times being linked, the rate constant bounds—calculated from the preexponential factors of the decay trace with $\tilde{b}_1 = 1$ and $\tilde{c}_1 = 1$, and the globally determined decay times—were identical with those when only the pivotal decay trace was analyzed.

8. Discussion

An intramolecular two-state excited-state process is not identifiable without any *a priori* information about the system parameters k_{ij}, $\tilde{b}_1$ and $\tilde{c}_1$. Decay curves collected at various excitation and/or emission wavelengths do not provide enough independent information. Additional information is required to identify the system.

When no information about the rate constants is available, bounds on all the rate constants can be specified using a decay trace with $\tilde{b}_1 = 1$ and $\tilde{c}_1 = 1$ or, equivalently, $\tilde{b}_1 = 0$ and $\tilde{c}_1 = 0$. Analysis of this decay with fixed $(\tilde{b}_1 = 1,\ \tilde{c}_1 = 1)$ or, equivalently, $(\tilde{b}_1 = 0,\ \tilde{c}_1 = 0)$ [or of a fluorescence decay surface which includes this decay with fixed $(\tilde{b}_1 = 1,\ \tilde{c}_1 = 1)$ or, equivalently, $(\tilde{b}_1 = 0,\ \tilde{c}_1 = 0)$] yields plateau values for S_1, S_2 and P within certain limits, on condition that one rate constant is kept constant at various values and the remaining system parameters are freely adjustable. These limits correspond to the lower and upper bounds on the scanned rate constant. It must be emphasized that the scanning procedure described here is not related to the search in parameter space to determine the confidence intervals of the parameters of an identifiable system [24]. The upper and lower bounds on the rate constants also can be derived analytically using the functions S_1, S_2 and P. Moreover, the expressions for the bounds can be rewritten in terms of decay times and preexponentials. This means that upper and lower limits on the rate constants can be specified from a biexponential analysis of a single decay curve with $\tilde{b}_1 = 1$ and $\tilde{c}_1 = 1$ or, equivalently, $\tilde{b}_1 = 0$ and $\tilde{c}_1 = 0$. Note that a biexponential decay with $\tilde{b}_1 = 1$ and $\tilde{c}_1 = 1$ or, equivalently, $\tilde{b}_1 = 0$ and $\tilde{c}_1 = 0$, is only possible when $P \neq 0$.

Finally, this analysis approach can provide kinetic information of intramolecular electron transfer and exciplex formation when no suitable model compound is available.

Acknowledgements

NB is an Onderzoeksleider of the Belgian Fonds voor Geneeskundig Wetenschappelijk Onderzoek (FGWO). LVD thanks the K.U. Leuven for financial assistance.

References

1 D.V. O'Connor and D. Phillips, Time-correlated single photon counting (Academic Press, London, 1984).
2 N. Boens, in: Luminescence techniques in chemical and biochemical analysis, eds. W.R.G. Baeyens, D. De Keukeleire and K. Korkidis (Marcel Dekker, New York, 1991) pp. 21–45.
3 J.R. Lakowicz, I. Gryczynski, G. Laczko, N. Joshi and M.L. Johnson, in: Luminescence techniques in chemical and biochemical analysis, eds. W.R.G. Baeyens, D. De

Keukeleire and K. Korkidis (Marcel Dekker, New York, 1991) pp. 141–177.
4 E. Gratton, J.R. Alcala and B. Barbieri, in: Luminescence techniques in chemical and biochemical analysis, eds. W.R.G. Baeyens, D. De Keukeleire and K. Korkidis (Marcel Dekker, New York, 1991) pp. 47–72.
5 J.R. Knutson, J.M. Beechem and L. Brand, Chem. Phys. Lett. 102 (1983) 501–507.
6 J.M. Beechem and L. Brand, Photochem. Photobiol. 44 (1986) 323–329.
7 L.D. Janssens, N. Boens, M. Ameloot and F.C. De Schryver, J. Phys. Chem. 94 (1990) 3564–3576.
8 N. Boens, L.D. Janssens and F.C. De Schryver, Biophys. Chem. 33 (1989) 77–90.
9 D.H. Anderson, Compartmental modeling and tracer kinetics, in: Lecture notes in biomathematics, vol. 50 (Springer-Verlag, Berlin, 1983).
10 J.A. Jacquez, Compartmental analysis in biology and medicine (Elsevier, Amsterdam, 1972).
11 J.M. Beechem, M. Ameloot and L. Brand, Chem. Phys. Lett. 120 (1985) 466–472.
12 M. Ameloot, J.M. Beechem and L. Brand, Chem. Phys. Lett. 129 (1986) 211–219.
13 M. Ameloot, N. Boens, R. Andriessen, V. Van den Bergh and F.C. De Schryver, J. Phys. Chem. 95 (1991) 2041–2047.
14 R. Andriessen, N. Boens, M. Ameloot and F.C. De Schryver, J. Phys. Chem. 95 (1991) 2047–2058.
15 M.M.H. Khalil, N. Boens, M. Van der Auweraer, M. Ameloot, R. Andriessen, J. Hofkens and F.C. De Schryver, J. Phys. Chem. 95 (1991) 9375–9381.
16 R. Andriessen, M. Ameloot, N. Boens and F.C. De Schryver, J. Phys. Chem. 96 (1992) 314–326.
17 V. Van den Bergh, N. Boens, F.C. De Schryver, M. Ameloot, A. Kowalczyk, Phys. Chem. 166 (1992) 249–258.
18 N. Boens, R. Andriessen, M. Ameloot, L. Van Dommelen and F.C. De Schryver, J. Phys. Chem. 96 (1992) 6331–6342.
19 N. Boens, M. Ameloot, B. Hermans, F.C. De Schryver and R. Andriessen, J. Phys. Chem. 97 (1993) 799–808.
20 A.L. Rabenstein, Elementary differential equations with linear algebra, 3rd edn. (Harcourt Brace Jovanovich, San Diego, CA, 1982).
21 D.W. Marquardt, J. Soc. Ind. Appl. Math. 11 (1963) 431–441.
22 B.T. Smith, J.M. Boyle, B.S. Garbow, Y. Ikeke, V.C. Klema and C.B. Moler, in: Matrix eigensystem routines—EISPACK Guide, eds. G. Goos and J. Hartmanis, Lecture notes in computer science, vol. 6 (Springer-Verlag, Berlin, 1974).
23 M. Van den Zegel, N. Boens, D. Daems and F.C. De Schryver, Chem. Phys. 101 (1986) 311–335.
24 J.M. Beechem, E. Gratton, M. Ameloot, J.R. Knutson, L. Brand, in: Topics in fluorescence spectroscopy, vol. 2: Principles, ed. J.R. Lakowicz (Plenum Press, New York, 1991) pp. 241–305.